Sieber, J., & Krauskopf, B. (2007). Tracking oscillations in the presence of delay-induced essential instability.

Tracking oscillations in the presence of delay-induced essential instability

J. Sieber [a,*] B. Krauskopf [b]

[a] *Department of Engineering, University of Aberdeen, Fraser Noble Building, King's College, Aberdeen AB24 3UE, United Kingdom*

[b] *Department of Engineering Mathematics, University of Bristol, Queen's Building, Bristol BS8 1TR, United Kingdom*

August 2007

Abstract

Hybrid experiments, which couple mechanical experiments and computer simulations bidirectionally and in real-time, are a promising experimental technique in engineering. A fundamental problem of this technique are delays in the coupling between simulation and experiment. We discuss this issue for a simple prototype hybrid experiment: a mechanical pendulum that is parametrically excited by coupling it to a simulated linear mass-spring-damper system. Under realistic conditions a small delay in the coupling can give rise to an essential instability. Namely, the linearization has infinitely many unstable eigenvalues for arbitrarily small delay. This type of instability is impossible to compensate for with any of the standard compensation techniques known in engineering.

We introduce an approach based on feedback control and Newton iterations and show that it is able to overcome the essential instability. The basic idea consists of two parts. First, we change the bidirectional coupling between experiment and computer simulation to a unidirectional coupling and stabilize the experiment with a feedback loop. Second, we place the modified hybrid experiment into a Newton iteration scheme. If the iteration converges then the hybrid experiment behaves just as the original emulated system (within the experimental accuracy). Using path-following, oscillations and their bifurcations can be tracked systematically without knowledge of an underlying model for the experiment.

Key words: hybrid testing, coupling delay, bifurcation analysis.

* Corresponding author.
Email addresses: J.Sieber@abdn.ac.uk (J. Sieber),
B.Krauskopf@bristol.ac.uk (B. Krauskopf).

1 Introduction

Nonlinear oscillations are a well-known feature of nonlinear dynamical systems. This type of self-sustained non-stationary behavior is often born in a Hopf bifurcation, where a stable steady-state loses its stability when two complex conjugate eigenvalues of its linearization cross the imaginary axis; see standard text books such as [1,2]. When a mathematical model of the system under consideration is known, for example, in the form of an ordinary differential equation (ODE), then the bifurcating nonlinear oscillation can be tracked, regardless of its dynamical stability, in a suitable parameter as a periodic solution of the ODE. Furthermore, the Hopf bifurcation itself, as well as other bifurcations (stability boundaries) of nonlinear oscillations, can be detected and tracked in two or more parameters. This tracking (one also speaks of path-following or numerical continuation) of different types of solutions and their bifurcations has emerged as a tremendously useful tool for the analysis of nonlinear dynamical systems. It can be performed with a number of freely available software packages; see, for example, the recent survey [3].

In this paper we consider the problem of tracking oscillations and stability boundaries directly in an experiment, that is, in a situation when a full mathematical model of the system under consideration is *not* available. More specifically, we are interested in hybrid testing experiments and, in particular, in *real-time dynamic substructured* testing of mechanical and civil engineering systems [4–7]. This term refers to the splitting of a complex structure into two components (in the simplest case). The first component, for which a reliable model is available, is simulated on the computer. The second component, typically the part that contains nonlinearities which are difficult to model reliably, is coupled bidirectionally and in real time to the computer model of the first component. The coupling in one direction is done by a transfer system (for example, a servo-mechanical actuator) that enforces the displacements computed in the numerical simulation onto the experimental component. To close the loop, the forces measured at the actuator are fed into the numerical simulation, where they enter as an inhomogeneity.

Section 2 explains the general hybrid setup using a concrete example: a substructured version of a nonlinear vibration damper in the form of a real pendulum that is coupled at its pivot to a computer simulation of a vertically excited mass-spring-damper (MSD) system; see Fig. 1. Throughout the paper we formulate all statements and algorithms for this prototype nonlinear hybrid experiment. Note that the original emulated pendulum-MSD system (a parametrically excited two-degree of freedom oscillator) can be modeled easily and shows a rich bifurcation structure. This makes the pendulum-MSD system an ideal test candidate for hybrid testing of nonlinear dynamical phenomena in general.

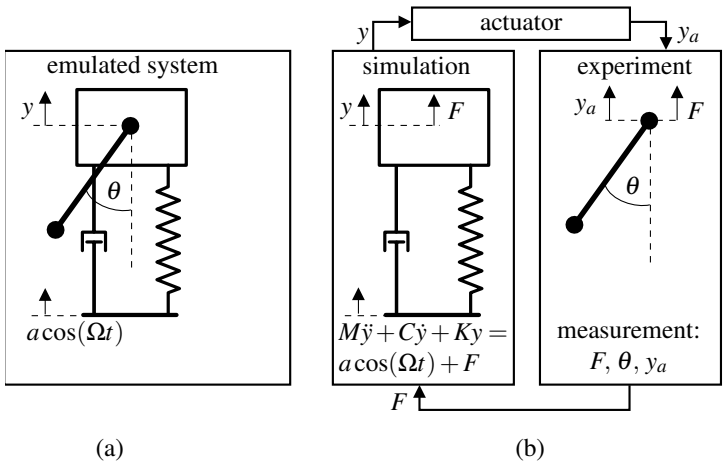

Fig. 1. Sketch of the decomposition of the overall pendulum-MSD system into a computer simulation of a mass-spring-damper system and a real pendulum. Panel (a) shows the original (emulated) system, and panel (b) the bidirectionally real-time coupled system as studied in [6,7], where the pendulum is of mass $m = 0.27\,\mathrm{kg}$ and length $l = 0.1955\,\mathrm{m}$.

One major issue in hybrid testing is the presence of unavoidable delays between the experimental part and the computer model, which may lead to instability of the coupled system. In many situations delay compensation techniques are able overcome this problem [5,7]. However, as we demonstrate in Section 3, for certain hybrid tests delays give rise to an essential instability, meaning that at the linear level the delay coupled system has infinitely many unstable eigenvalues regardless of the size of the delay. Section 3 and Section 4 show for the hybrid pendulum-MSD system how the instability arises and why it persists even when one applies delay compensation.

The centerpiece of our paper is Section 5 where we show how the delay-induced essential instability can be overcome in the context of bifurcation analysis for experiments [8,9] (as is explained for the hybrid pendulum-MSD system in Fig. 1). Its basic elements are:

(B1) decoupling the actuator from the computer simulation and drive it with a periodic signal $\tilde{y}(t)$ instead. Now the hybrid system is only unidirectionally coupled but has an additional periodic input $\tilde{y}(t)$.

(B2) adding a stabilizing feedback loop with a periodic control demand $\tilde{\theta}(t)$ to the experimental component. In the pendulum-MSD example this should be a proportional-plus-derivative control PD$[\theta - \tilde{\theta}]$ depending on the angle $\theta(t)$ of the pendulum.

(B3) The hybrid system is stable after the modifications (1) and (1) but has two additional periodic inputs: $\tilde{\theta}(t)$ and $\tilde{y}(t)$. Whatever periodic input $(\tilde{\theta}(t), \tilde{y}(t))$ we choose, the output $y_a(t)$ (the motion of the actuator), $\theta(t)$ (the motion of the angle), and $y(t)$ (the output of the simulation) will settle to a periodic state of the same period after a short transient.

(B4) If the conditions

$$y(t) = y_a(t) \quad \text{and} \quad \theta(t) = \tilde{\theta}(t) \tag{1}$$

are satisfied then the partially decoupled and feedback controlled system reproduces the original emulated system perfectly. The first condition guarantees synchronization between the simulation and the motion of the actuator. The second condition makes the feedback control non-invasive.

(B5) The conditions in Eq. (1) depend nonlinearly but smoothly on the inputs $\tilde{\theta}$ and $\tilde{y}$. Together, the conditions define the inputs $\tilde{\theta}$ and $\tilde{y}$ (locally) uniquely and can be solved by a Newton iteration.

(B6) embedding the Newton iteration into a path-following procedure guarantees its convergence. It is then also Possible to extend the nonlinear system Eq. (1) by bifurcation conditions to track bifurcations in two or more system parameters.

Control-based bifurcation analysis as defined by steps (B1)–(B6) has several practical advantages. First of all, ut does not require an underlying model of the overall dynamical system. Instead it relies on feedback stabilizability of the experimental component, which is generally a mild assumption in the context of a hybrid test. Moreover, we do not need to set the initial conditions for the experimental component, which would be difficult in practice. The Newton iteration and the path-following in the steps (B5) and (B6) do not have to be performed in real time. Also, the simulation of the numerical model does not have to be performed in real time anymore. Only the feedback loop for the experiment in step (B2) has to meet real-time requirements. Finally, as we will show in Secs. 5 and 6, control-based bifurcation analysis is able to deal with delay-induced essential instabiliy of the hybrid system.

Section 6 presents a feasibility study where we use a computer experiment of the pendulum with noise and limited measurement accuracy to track the stability boundary of the hanging-down state of the pendulum-MSD system, as well as a family of periodic solutions. Control-based bifurcation analysis of the actual hybrid pendulum-MSD system is work in progress, because the experimental setup from [6,7] requires a modification (the addition of a feedback loop). Finally, in Section 7 we draw some conclusions and point out future work.

2 Pendulum-MSD system as a prototype hybrid experiment

Hybrid test experiments — also called substructured experiments — aim to test large structures by coupling a critical, nonlinear or poorly understood component to a real-time simulation of a numerical model of the remainder of the structure [4,10]. This critical component can be, for example, a support cable of a bridge, or a damper that keeps helicopter blades apart.

The typical setup of a hybrid experiment is sketched in Fig. 1 for the simple prototype experiment that we consider: a pendulum that is attached to a linear vertically excited mass-spring-damper (MSD) system; see Fig. 1(a). The pendulum-MSD system is a parametrically excited oscillator with a geometric nonlinearity and two degrees of freedom, and a prototype system for parametric resonance phenomena as they occur, for example, in bridge cables [6]. The pendulum-MSD system also acts as a nonlinear vibration damper for the vertical motion of the mass. Throughout the paper we will formulate all statements and algorithms for the pendulum-MSD example, which can be modeled mathematically as

$$M\ddot{y} + C\dot{y} + Ky = a\cos(\Omega t) - m\ddot{y} - ml\left[\ddot{\theta}\sin\theta + \dot{\theta}^2\cos\theta\right], \quad (2)$$

$$\ddot{\theta} + \frac{\kappa}{ml^2}\dot{\theta} + \left[\frac{g+\ddot{y}}{l}\right]\sin\theta = 0. \quad (3)$$

Here θ is the angular displacement of the pendulum, y is the vertical displacement of the pendulum pivot that is attached to the mass, M, C and K are the mass, damping and stiffness of the MSD system, m is the mass of the pendulum, l is the length of the pendulum, g is the acceleration due to gravity, and a and Ω are the amplitude and the frequency of the forcing. A force amplitude of a corresponds to a displacement excitation of amplitude $a/\sqrt{\Omega^2C^2 + K^2}$ of the MSD.

The pendulum-MSD system has a rich but well understood bifurcation structure. For the mathematical model (2)–(3) all bifurcations of periodic orbits (period doubling, symmetry breaking, torus and saddle-node bifurcations, homoclinic and heteroclinic tangencies) can be explored systematically with numerical continuation methods as implemented in AUTO [11]; see also [2,12] for more background information on numerical continuation. The pendulum-MSD system is an ideal prototype example for hybrid testing and experimental bifurcation analysis, because it is possible to compare the results of the hybrid experiment to a reliable model over a range of different dynamical phenomena.

The decomposition of the pendulum-MSD system into a simulation and a real experiment is shown in Fig. 1(b). In this setup that was realized in [6,7] !!!!, the mechanical part of the hybrid experiment is a pendulum of mass $m = 0.27\,\mathrm{kg}$ and length $l = 0.1955\,\mathrm{m}$. The linear viscous friction coefficient κ was estimated as $7.5 \cdot 10^{-3}\,\mathrm{kg/s}$ from the results in [7]. The pendulum is attached at its pivot to a transfer system, which was a mechanical actuator in the experiment. The transfer system is provided with a trajectory $y(t)$ for its vertical motion, which is calculated by numerical simulation of the linear MSD system

$$M\ddot{y} + C\dot{y} + Ky = a\cos(\Omega t) + F(t). \quad (4)$$

The numerical model (4) has an inhomogeneity $F(t)$ that originates from force measurements at the pivot of the pendulum. This means that the hybrid

experiment involves a loop between three stages:

(H1) the numerical simulation of model (4) with input $F(t)$;
(H2) the transfer via the actuator of the output $y(t)$ of the simulation; and
(H3) feeding back the force measurement $F(t)$ to the simulation.

All parts of the loop need to be implemented in real time, and need to run in parallel to the experiment. One advantage of the hybrid setup is that one can easily and systematically vary the system parameters of the numerical subsystem (a, Ω, M, C and K in our case), while testing the nonlinear structure (the pendulum) experimentally and in its original size.

3 Essential instability due to delay in the coupling

The real-time coupling between simulation and experiment via a transfer system and force measurements introduces a number of difficulties. Apart from the inherent noisiness of the force measurements, the most severe problem is the mismatch between the prescribed trajectory $y(t)$ obtained from the simulation and the output $y_a(t)$ of the transfer system; see Fig. 1(b). This mismatch is referred to as the *synchronization error*

$$e(t) = y_a(t) - y(t). \tag{5}$$

Since the output of the simulation $y(t)$ is known, the synchronization error can be determined in a hybrid experiment by recording the actual motion $y_a(t)$ of the transfer system (the mechanical actuator). Generally, the smallness of the synchronization error $e(t)$ is taken as a measure of accuracy of the whole hybrid experiment [5,13]. In many situations it is a good modeling assumption to say that the actual trajectory $y_a(t)$ of the actuator follows the prescribed trajectory $y(t)$ exactly, but with a fixed small pure time delay τ [6,13,14], hence,

$$y_a(t) = y(t - \tau). \tag{6}$$

This idealization of the actuator is a modeling assumption. It is supported by two facts. First, using (6) in the mathematical model, system (2)–(3) in the case of the pendulum-MSD system, leads to a mathematical model in the form of a delay differential equation (DDE; see Eq. (7) below). For the case $m < M$ the DDE model predicts instability of the hybrid experiment for delays larger than a certain critical delay τ_c; see [6]. The experimental observations confirmed this prediction of instability and even showed a precise quantitative agreement with the predicted values of the critical delays τ_c and the predicted frequency of the growing vibration. This type of agreement was demonstrated not only for the pendulum-MSD system but also for other prototype experiments for which models are available, such as other multi-MSD

hybrid experiments [6,13,15]. Second, the delay compensation techniques developed on the basis of assumption (6) in [5,14,16] have been successful in suppressing these instabilities and reducing the synchronization error $e(t)$ significantly, for example, in the studies [5,7]. One underlying assumption behind the modeling assumption (6) is that the modulus of the force $F(t)$ is moderate, meaning that it has a negligible influence on the actuator.

Specifically for the pendulum-MSD system considered here, inserting (6) into (2)–(3) gives (see [6])

$$\begin{aligned} M\ddot{y} + ml\sin\theta\ddot{\theta} + m\ddot{y}(t-\tau) + C\dot{y} + Ky + ml\dot{\theta}^2\cos\theta &= a\cos(\Omega t), \\ \ddot{\theta} + \frac{\kappa}{ml^2}\dot{\theta} + \frac{1}{l}[g + \ddot{y}(t-\tau)]\sin\theta &= 0, \end{aligned} \tag{7}$$

where we have dropped the argument t for all dependent variables, except for those that feature the delay τ. The fact that system (7) has terms that depend on the state some time τ ago has some important consequences. The state space of (7) is infinite-dimensional: the evolution depends on the history of $\dot{y}$ in the time interval $[t-\tau, t]$. What is more, the delay actually enters in the highest derivative $\ddot{y}(t-\tau)$ of y, which means that (7) is an example of a *neutral* delay differential equation [17]. As we will see now, this neutrality is the reason why system (7) shows an extreme instability if $m > M$ near angles $\theta = 0$ or π for arbitrarily small delay τ.

Our first step is to bring (7) into the standard form used in the textbooks [17,18], which allows us to determine which kind of initial conditions for $\dot{y}$ makes $\ddot{y}(t-\tau)$ a well defined object. This step is quite technical, but it allows us to clarify in which sense (7) is a well-posed initial-value problem for a dynamical system, and how one can determine the stability properties of linearizations along trajectories of (7). To this end, we rewrite (7) as an explicit first-order system consisting of a difference equation and an ODE. Let us denote the components of the first-order system by (u, θ, y, v, w) where $u([t-\tau, t])$ is the history segment of $\dot{y}$, v is an auxiliary scalar variable, and w is a modification of $\dot{\theta}$. The evolution of (u, θ, y, v, w) that is equivalent to (7) is given by

$$u(t) = \left[-\frac{m}{M}\cos^2\theta(t)\right]u(t-\tau) + \frac{1}{M}v(t), \tag{8}$$

$$\dot{y}(t) = u(t), \tag{9}$$

$$\dot{\theta}(t) = w(t) - \frac{\sin\theta(t)}{l}, \tag{10}$$

$$\dot{v}(t) = f_1(t, u(t), u(t-\tau), \theta(t), y(t), \dot{\theta}(t)), \tag{11}$$

$$\dot{w}(t) = f_2(u(t), u(t-\tau), \theta(t), \dot{\theta}(t)), \tag{12}$$

where the functions f_1 and f_2 are

$$\begin{aligned} f_1(t,u_0,u_1,\theta,y,\dot\theta) &= \frac{\kappa}{l}\dot\theta\sin\theta + mg\sin^2\theta - Cu_0 - Ky + a\cos(\Omega t) \\ &\quad - ml\dot\theta^2\cos\theta - m\dot\theta\sin(2\theta)u_1, \\ f_2(u_0,u_1,\theta,\dot\theta) &= -\frac{\kappa}{ml}\dot\theta - \frac{g}{l}\sin\theta + \frac{1}{l}\dot\theta\cos\theta\, u_1. \end{aligned}$$

In the right-hand-sides of (11) and (12) one can substitute $\dot\theta$ by using (10), which gives a well-defined set of equations (8)–(12) for (u,θ,y,v,w). The solution of this set of equations on an interval $(t_1,t_1+\tau]$ is uniquely defined by the variation-of-constants formulation of (8)–(12); see [19].

The appropriate initial condition $\mathbf{x}$ (over the delay interval) consists of one function segment $u([t_1-\tau,t_1])$ and the four scalars $y(t_1)$, $\theta(t_1)$, $v(t_1)$ and $w(t_1)$. Note that the trajectory of u is only continuous in t_1 if (8) is satisfied for the initial condition $\mathbf{x}$. If we require continuity for u this effectively gives a nonlinear condition on the initial condition of the auxiliary variable v. Only such continuous velocities are physically relevant, but note that system (8)–(12) can actually also be solved for square-integrable functions u.

The theory for systems composed of difference equations and ODEs is well developed; see, for example, the text books [17,18]. It is known that the time map $\mathbf{X}(t_2,t_1;\mathbf{x})$, given by the evolution of (8)–(12) from time t_1 to time t_2 starting from the initial condition $\mathbf{x}$, is smooth with respect to its argument $\mathbf{x}$ (the initial condition) whenever the right-hand-sides are smooth functions. We denote the derivative of $\mathbf{X}$ with respect to its third argument by $\partial_3\mathbf{X}$. It can be computed by solving the variational equations for (8)–(12).

Now we show that the time map $\mathbf{X}$ depends extremely sensitively on its initial condition $\mathbf{x}$ when passing through a hanging down state $\theta=0$. This dependence is determined by the spectrum of the linear map $\partial_3\mathbf{X}(t_1+\delta,t_1;\hat{\mathbf{x}}_*)$. Let us denote the trajectory of $\mathbf{X}$ on the interval $[t_1,t_1+\delta]$ starting from $\hat{\mathbf{x}}_*$ by

$$\mathbf{x}_*(t) = [u_*(t),\theta_*(t),y_*(t),v_*(t),w_*(t)] \quad \text{for} \quad t\in[t_1,t-1+\delta]),$$

where $\theta_*(t_1)=0$, $\mathbf{x}_*(t_1)=\hat{\mathbf{x}}_*$, and the solution of the variational equations for system (8)–(12) on $[t_1,t_1+\delta]$ by

$$\mathbf{x}(t) = [u(t),\theta(t),y(t),v(t),w(t)]\,.$$

The variational equation of (8) reads

$$u(t) = \left[-\frac{m}{M}\cos^2\theta_*(t)\right]u(t-\tau) + \frac{1}{M}v(t) + \left[\frac{m}{M}\sin(2\theta_*(t))u_*(t-\tau)\right]\theta(t), \quad (13)$$

while the variational equations for θ, y, v and w are linear ODEs depending on $u(t)$ and $u(t-\tau)$. The theory developed in [17] implies that the time

map $\partial_3 \mathbf{X}(t_1+\delta, t_1; \hat{\mathbf{x}}_*)$ has (countably) infinitely many eigenvalues λ_j ($j = -\infty, \ldots, \infty$) and that

$$|\lambda_j| \to \rho \text{ for } |j| \to \infty \tag{14}$$

where ρ is the essential spectral radius of the time map from t_1 to $t_1+\delta$ of the linear difference equation

$$u(t) = \left[-\frac{m}{M}\cos^2\theta_*(t)\right] u(t-\tau). \tag{15}$$

If $m > M$ and $\delta > 0$ is sufficiently small then the prefactor of $u(t-\tau)$ in (15) satisfies

$$\left|-\frac{m}{M}\cos^2\theta_*(t)\right| > \rho_0 \tag{16}$$

for some $\rho_0 > 1$ (because $\theta_*(t_1) = 0$). Thus, the essential spectral radius ρ of the time map $t_1 \to t_1+\delta$ for the difference equation (15) satisfies

$$\rho \geq (\rho_0)^{\delta/\tau}. \tag{17}$$

The right-hand-side of estimate (17) is larger than one for arbitrarily small delays τ. Even more, it grows strongly for $\tau \to 0$. Equation (14) implies that, at least for time δ, the linearization along any trajectory of (8)–(12) passing through $\theta = 0$ (or π) has infinitely many eigenvalues with modulus greater or equal to $(\rho_0)^{\delta/\tau}$, which due to (16) is dramatically larger than 1 for $m > M$. Consequently, any small disturbance occurring in the hybrid experiment will be amplified to order 1 whenever θ is close to 0 or π. The fact that infinitely many eigenvalues and the essential spectral radius of the linearization are larger than 1 motivates our notion of referring to this case as an *essential instability*.

Remark The frequencies corresponding to the unstable eigenvalues have (asymptotically) a spacing of $2\pi/\tau$. Thus, most of the unstable eigenvalues occur at very large frequencies. A real mechanical actuator is not capable of supporting an instability at infinitely many frequencies. Typically, the actuator will be a stiff approximation of the idealization (6), for example,

$$\ddot{y}_a + 2\omega_s\dot{y}_a + \omega_s^2[y_a - y(t-\tau)] = F/m_a \tag{18}$$

for a large positive ω_s where F is the force measured at the pivot and m_a is the mass of the actuator. This gives rise to a regularization of the ill-posed problem (15), which nevertheless has a large number of strongly unstable eigenvalues for large ω_s and small delays. Hence, the essential instability renders the hybrid test practically infeasible for $m > M$ also for a real actuator rather than an idealized one.

4 Failure of classical delay compensation

The delay compensation methods developed in [5,14] and applied in [5,7] are not able to overcome the essential instability discussed in Section 3. The choice of delay compensation methods for hybrid experiments is more restricted than in the classical field of delay compensation for feedback control where many more approaches have been proved to work; see, for example, [20–22]. The reason behind this restriction is that the hybrid system with compensation not only has to be stable, but it also needs to approximate the unknown dynamics of the emulated system — namely (2)–(3) in our case.

The two methods developed in [5,14] are based on polynomial extrapolation. This means that the input for the actuator is not $y(t)$ but $P[y](t+\hat{\tau})$ where $P[y]$ is an interpolation polynomial obtained from a history segment of y, where $\hat{\tau}$ is an estimate of the delay time. In [5] $\hat{\tau}$ is adapted along the trajectory and the polynomial P is the second- or fourth-order least-squares fitting polynomial of $(y(t-k\Delta),\ldots,y(t))$ where Δ is the step size of the numerical simulation (which is equal to the sampling time of the experiment). Thus, in the actuator model (6) the term $y(t-\tau)$ is replaced by $P[y(\cdot-\tau)](t+\hat{\tau})$. Because the evaluated least-squares fitting polynomial is a linear combination of the interpolated values of y, the term $y(t-\tau)$ in (7) is effectively replaced with a linear combination of past terms of y of the form

$$P[y(\cdot-\tau)](t+\hat{\tau}) = c_0 y(t-\tau) + \ldots c_k y(t-\tau-k\Delta). \tag{19}$$

One condition on the polynomial extrapolation (in fact, of any delay compensation scheme) is consistency, which means that

$$c_0 + \ldots + c_k = 1. \tag{20}$$

Only the consistency condition (20) guarantees that the compensation is accurate at least for $\hat{\tau} = \tau = 0$. Inserting the compensation (19) into system (8)–(12) for the hybrid experiment we obtain a neutral delay differential equation that has as its essential part the difference equation

$$u(t) = \left[-\frac{m}{M}\cos^2\theta_*(t)\right][c_0 u(t-\tau) + \ldots c_k u(t-\tau-k\Delta)] \tag{21}$$

with $c_0 + \ldots + c_k = 1$. Instead of the single small delay τ in the essential part (15) the difference equation (21) has multiple delays, τ up to $\tau + k\Delta$. Typically, all of these delays are small ($\tau \sim 10\,\text{ms}$, $\Delta = 1\,\text{ms}$). Computing the essential spectral radius of the time map $t_1 \to t_1 + \delta$ for (21) analytically is difficult. However, the theory of neutral equations [17] states that for any difference equation of the form

$$u(t) = d_0 u(t-\tau_0) + \ldots + d_k u(t-\tau_k) \quad \text{where } |d_0| + \ldots + |d_k| > \rho_0 \tag{22}$$

there exists a $(k+1)$-tuple of delays $[\tilde{\tau}_0, \ldots, \tilde{\tau}_k]$ arbitrarily close to $[\tau_0, \ldots, \tau_k]$ such that the essential spectral radius of the time-δ map of

$$u(t) = d_0 u(t - \tilde{\tau}_0) + \ldots + d_k u(t - \tilde{\tau}_k)$$

is larger than $(\rho_0)^{\delta/\tau_k}$. This also holds for time-dependent coefficients $d_0, \ldots, d_k$. For a consistent delay compensation scheme this implies that the scheme is uncontrollably sensitive with respect to the delays $\tau, \ldots, \tau + k\Delta$ whenever the hybrid system (7) is essentially unstable in our sense, that is, whenever condition (16) is satisfied. In other words, any delay compensation scheme applied to a system with an essential instability will also have an essential instability.

There is a physical reason for the essential instability of the pendulum-MSD system. Namely, the two subsystems are coupled at a fixed joint (in contrast to a spring), while one is prescribing displacements and measuring forces at the interface; see Fig. 1 (b). If $M < m$ (or the coupling is via a spring) then instabilities can still occur but they involve only a small number of eigenvalues when the delay is small (typically $\approx 10\,\text{ms}$). Hence, classical delay compensation is suitable for these non-essential instabilities [5]. However, as we have seen, for $m > M$ delay compensation fails for any delay $\tau > 0$.

As a consequence, for a mass ratio $m/M > 1$ it is impossible to achieve an approximation of the dynamics of the emulated system (2)–(3) of Fig. 1 (a) by a hybrid experiment with bidirectional real-time coupling as in Fig. 1 (b). Any trajectory of the emulated system (2)–(3) will eventually spend some time δ near $\theta = 0$ or π (the time δ is considerably larger than $\tau \approx 10\,\text{ms}$). During this time the essential instability of the linearized time map $\partial_3 X$ amplifies any small disturbances within the hybrid experiment to order 1.

5 Interface matching by Newton iteration

As we demonstrate now, it is still possible to perform a systematic analysis of the dynamics of the emulated system of Fig. 1(a) by studying the hybrid system. To this end, we break the coupling in one direction, match the output at the interface by a Newton iteration and exploit some fundamental ideas from bifurcation theory.

Fig. 2 shows how the coupling between the two subsystems is relaxed by breaking the bidirectional coupling. Instead, the actuator is fed with a periodic demand $\tilde{y}(t)$ (for example, we choose the period $4\pi/\Omega$ in Section 6). After this modification the experimental component is a parametrically (periodically) excited pendulum. The force output $F(t)$ of the experiment still enters the

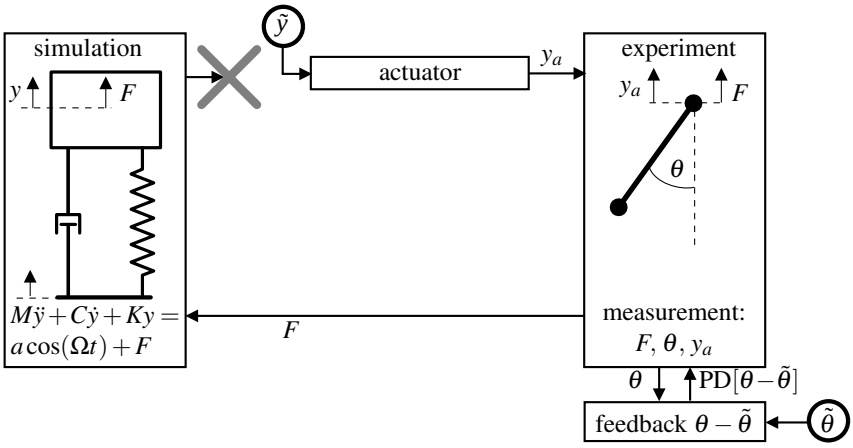

Fig. 2. Sketch of the iterative hybrid experiment. The periodic input $\tilde{y}$ replaces the coupling from the simulation to the experiment. Additionally, a classical (proportional-plus-derivative) feedback loop stabilizes the parametrically driven pendulum. The system has two additional periodic inputs: $\tilde{\theta}$, $\tilde{y}$ (in black circles). A model for this setup is system (4), (29), (30).

simulation. In addition, we stabilize the parametrically excited pendulum by a classical feedback loop (for example, with proportional-plus-derivative control) with a periodic demand signal $\tilde{\theta}(t)$ (also of period $4\pi/\Omega$):

$$\mathrm{PD}[\theta-\tilde{\theta}](t) = k_1[\theta(t-\tau)-\tilde{\theta}(t-\tau)] + k_2[\dot{\theta}(t-\tau)-\dot{\tilde{\theta}}(t-\tau)] \tag{23}$$

(see Section 6 for the choice of control gains k_1 and k_2).

With these two modifications the hybrid system is only unidirectionally coupled and feedback-stabilized. For any pair of inputs $(\tilde{\theta}, \tilde{y})$ of period $4\pi/\Omega$ the outputs $\theta(t)$, $y(t)$ and $y_a(t)$ of this system have also period $4\pi/\Omega$ after a short transient (if the delay τ is small). Moreover, the output (θ, y, y_a) depends smoothly on the input $(\tilde{\theta}, \tilde{y})$ and all parameters. Whenever we find an input $(\tilde{\theta}, \tilde{y})$ of period $4\pi/\Omega$ such that the output satisfies for all times the conditions

$$0 = \theta(t) - \tilde{\theta}(t) \tag{24}$$
$$0 = y_a(t) - y(t) \tag{25}$$

then the trajectory of the partially decoupled and stabilized system in Fig. 2 is identical to an oscillation of period $4\pi/\Omega$ of the original emulated system in Fig. 1(a). Condition (24) implies that the actual control effort is zero, that is, the feedback control is non-invasive. Condition (25) guarantees that the synchronization error is zero. The right-hand-sides of (24) and (25) are two periodic functions that depend nonlinearly but smoothly on the two variables (also periodic) inputs $\tilde{\theta}$ and $\tilde{y}$ and on all system parameters.

As a consequence, it is possible to employ a Newton iteration to find inputs $\tilde{\theta}$ and $\tilde{y}$ satisfying the conditions (24) and (25). The Newton iteration is able

to solve systems of equations of the form

$$0 = \mathbf{F}(\mathbf{z}) \tag{26}$$

for a smooth vector-valued nonlinear function $\mathbf{F}$ (the *residual*) and a vector $\mathbf{z}$ by applying the iteration

$$\mathbf{z}_{l+1} = \mathbf{z}_l - (\mathbf{F}'_l)^{-1}\mathbf{F}(\mathbf{z}_l), \tag{27}$$

where $\mathbf{F}'_l$ is an approximation of the Jacobian of $\mathbf{F}$ in $\mathbf{z}_l$. In our case the variable $\mathbf{z}$ is the periodic vector function $(\tilde{\theta}, \tilde{y})$ and the residual $\mathbf{F}$ is the right-hand-side of (24)–(25), which is also periodic. In practice, we project $(\tilde{\theta}, \tilde{y})$ and the residual onto the leading m Fourier modes to obtain a finite-dimensional vector $\mathbf{z}$ and residual $\mathbf{F}$. If the function $\mathbf{F}$ is not analytically known (as is the case for (24)–(25)) the matrix $\mathbf{F}'_l$ has to be obtained either by a finite difference approximation or by a recursion. We use here the Broyden rank-1 update [23] given by

$$\mathbf{F}'_{l+1} = \mathbf{F}'_l + \frac{(\mathbf{F}(\mathbf{z}_l) - \mathbf{F}(\mathbf{z}_{l-1})) - \mathbf{F}'_l[\mathbf{z}_l - \mathbf{z}_{l-1}]}{(\mathbf{z}_l - \mathbf{z}_{l-1})^T(\mathbf{z}_l - \mathbf{z}_{l-1})}(\mathbf{z}_l - \mathbf{z}_{l-1})^T.$$

Thus, we can apply the Newton iteration even if we do not know an analytical expression for $\mathbf{F}$. All that is required is a good initial guess $\mathbf{z}_0$ and the ability to evaluate the residual $\mathbf{F}$ at a sequence of points $\mathbf{z}_l$ given by the recursion (27).

One evaluation of $\mathbf{F}$ in a point $\mathbf{z} = (\tilde{\theta}, \tilde{y})$ involves the following procedure.

(F1) Set the periodic function $\tilde{\theta}(t)$ as the control target in the feedback control (23) and the periodic function $\tilde{y}(t)$ as the actuator input. Both have period $4\pi/\Omega$.

(F2) Wait until the experiment has settled to a periodic output of period $4\pi/\Omega$ and measure the (periodic) outputs $\theta(t)$, $y(t)$ and $y_a(t)$. Use these outputs to evaluate the right-hand-sides of (24)–(25).

(F3) Project the right-hand-sides of (24)–(25) onto the first m Fourier modes to obtain $\mathbf{F}$.

This iterative procedure does not require any knowledge of the underlying model for the experimental component of the hybrid system in Fig. 2, nor do we need a model for the dependence of the actuator output y_a on the force F and the prescribed trajectory $\tilde{y}$ (say, (6) or (18)).

The problem of finding a good initial guess $\mathbf{z}_0$ can be solved by embedding the Newton iteration into a path-following procedure as described in [2,12]. We extend $\mathbf{z}$ by a system parameter (for example, $\mathbf{z} = (\tilde{\theta}, \tilde{y}, a)$). This gives a curve of solutions for (26) that corresponds to a one-parameter family of periodic motions of the original emulated system in Fig. 1(a). One can trace

out this solution curve by extending the nonlinear system (26) with the *pseudo-arclength condition*

$$\mathbf{z}_{\tan}^T[\mathbf{z} - \mathbf{z}_{\text{old}}] = s \tag{28}$$

where $\mathbf{z}_{\text{old}}$ is the previous point on the curve, $\mathbf{z}_{\tan}$ is an approximation to the tangent at the curve in $\mathbf{z}_{\text{old}}$ ($\mathbf{z}_{\tan}$ can be any unit vector that is not orthogonal to the curve) and s is a small parameter determining the step size along the curve. The solution of (26) extended by (28) gives the next point along the curve. A good initial guess for the Newton iteration is $\mathbf{z}_0 = \mathbf{z}_{\text{old}} + s\,\mathbf{z}_{\tan}$. A good starting point for the curve is, in this example, a solution that is harmonic in $\tilde{y}$ and 0 in $\tilde{\theta}$ (see Section 6). The embedding into a one-parameter family guarantees that the Newton iteration converges for small s as long as the solution curve is regular [12]. It also guarantees that the transients in step 5 of the evaluation of the residual $\mathbf{F}$ are short and that the method can be applied even if the feedback control achieves only local stabilization.

6 A case study of periodic orbit continuation

In this section we demonstrate which kind of questions about the dynamics of the emulated system can be answered when using the approach introduced in Section 5. In the spirit of a proof of concept, in all demonstrations in this section the experimental part of the system is evaluated by a separate computer simulation of

$$\ddot{\theta} + \frac{1}{l}\sin\theta\,\ddot{y}_a + \frac{\kappa}{ml^2}\dot{\theta} + \frac{g}{l}\sin\theta = -\,\mathrm{PD}[\theta - \tilde{\theta}](t) \tag{29}$$

(assuming torque control for the feedback to the pendulum, and choosing $k_1 = 4\,\mathrm{N/m}$, $k_2 = 4\,\mathrm{kg/s}$) with the idealized actuator model $y_a(t) = \tilde{y}(t - \tau)$ for $\tau = 10\,\mathrm{ms}$ and the force

$$F(t) = \; -m\ddot{y}_a - ml\left[\ddot{\theta}\sin\theta + \dot{\theta}^2\cos\theta\right] \tag{30}$$

as inhomogeneity in (4). We also take the limited accuracy into account, namely, we use only three relevant digits of the evaluations of the residual in (24)–(25).

Period doubling of hanging-down state In the original emulated system (2)–(3) the hanging-down state $\theta = 0$ loses its dynamical stability in a period doubling bifurcation. Standard bifurcation theory states that near this loss of stability a solution with a small harmonic amplitude of the angle θ and period $4\pi/\Omega$ emerges [2]. Hence, in order to find the boundary of stability of the hanging-down state it is sufficient to track small period-two solutions.

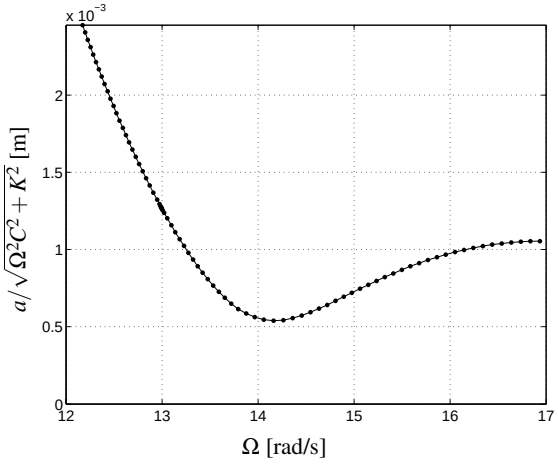

Fig. 3. Continuation of the period-doubling yields a stability curve in the two-parameter plane of Ω vs. the amplitude $a/\sqrt{\Omega^2C^2+K^2}$. Dots along the curve mark the steps of the continuation. Parameters of the simulated subsystem are $C = 0.1\,\mathrm{kg/s}$, $K = 200\,\mathrm{N/m}$, $M = 0.2\mathrm{kg}$; parameters of the pendulum are $m = 0.27\,\mathrm{kg}$, $l = 0.1955\,\mathrm{m}$ $\kappa = 7.5 \cdot 10^{-3}\mathrm{kg/s}$, delay $\tau = 10^{-2}\,\mathrm{s}$; control gains are $k_1 = 4\,\mathrm{N/m}$, $k_2 = 4\,\mathrm{kg/s}$; the amplitude of small angular oscillation is $r = 0.1\,\mathrm{rad}$.

We choose the vector of variables $\mathbf{z} = (\tilde{\theta}_1, \tilde{y}_1, a, \Omega)$ where $\tilde{\theta}_1(t) = \tilde{\theta}(\Omega t/(4\pi))$, $\tilde{y}_1(t) = \tilde{y}(\Omega t/(4\pi))$ (where we scale the periodic components of $\mathbf{z}$ to period 1). As $\mathbf{z}$ has one additional component Ω we append (26), (28) by the bifurcation condition

$$\int_0^1 \left[\tilde{\theta}_1(t)\right]^2 \mathrm{d}t = r^2 \tag{31}$$

for a small fixed r (which fixes the amplitude of the angle θ of the period-two solutions). The system (26), (28), (31) defines a sequence of points along the approximate (because $r > 0$) period-doubling bifurcation curve in which the hanging-down state $\theta = 0$ of the emulated system (2)–(3) loses its stability. Since (28) and (31) are known analytically, we we also know the corresponding rows of the Jacobian F' in (26) analytically. We approximate the two periodic functions $\tilde{\theta}_1$ and $\tilde{y}_1$ by their first two Fourier modes

$$\begin{aligned}\tilde{y}_1(t) &= y_0 + y_1 \exp(2\pi i t) + y_2 \exp(4\pi i t),\\ \tilde{\theta}_1(t) &= \theta_0 + \theta_1 \exp(2\pi i t) + \theta_2 \exp(4\pi i t),\end{aligned}$$

where $y_0, \theta_0 \in \mathbb{R}$, y_1, y_2, θ_1, $\theta_2 \in \mathbb{C}$. After a Galerkin projection onto these two Fourier modes, (24)–(25), together with (31), form a system of eleven (real-valued) equations for twelve (real-valued) variables. It implicitly defines a curve that can be traced by the path-following method described in Section 5. The curve of period-doublings thus obtained is shown in Fig. 3.

Since r is not zero but small and positive the computed curve is shifted slightly into the region of stability of the hanging-down state whenever the emerging $4\pi/\Omega$-periodic solutions are unstable (*subcritical* period doubling). Similarly,

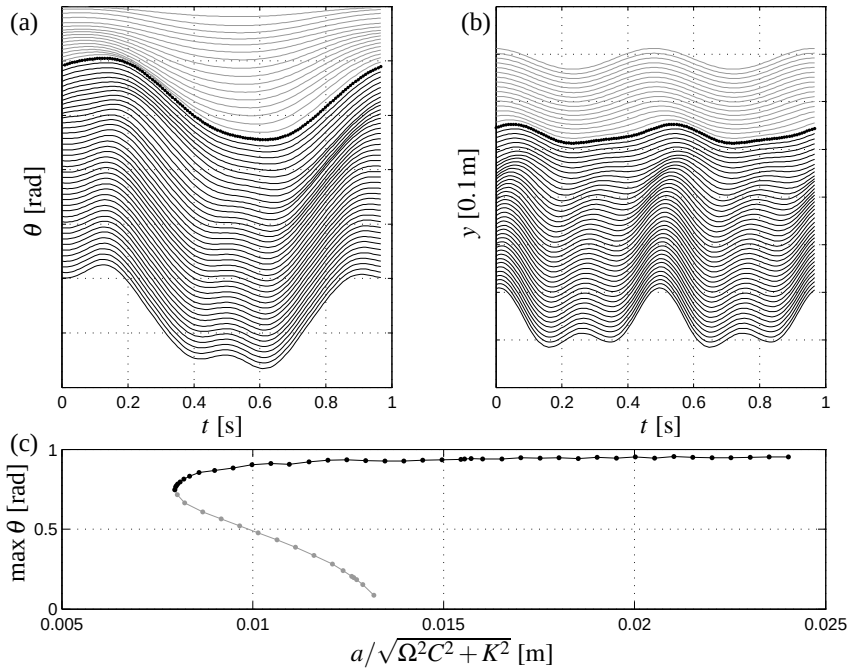

Fig. 4. One-parameter continuation for $\Omega = 13\,\mathrm{rad/s}$. Shown are time profiles of $\tilde{\theta}$ (a) and of $\tilde{y}$ (b) in a waterfall plot, and the one-parameter bifurcation diagram (c). Time profiles corresponding to unstable periodic orbits are gray, and time profiles corresponding stable periodic orbits are black; the saddle-node orbit in between the two cases, which corresponds to the fold point in panel (c), is shown in boldface. The label of the vertical axis in the panels (a) and (b) corresponds to the distance between horizontal grid lines.

it is shifted slightly into the region of instability whenever the emerging $4\pi/\Omega$-periodic solutions are stable (*supercritical* period doubling). The size of the shift is of the order $O(r^2)$.

Symmetric periodic orbits Fig. 4 shows the one-parameter family of symmetric $4\pi/\Omega$-periodic orbits branching off from the period doubling curve for fixed $\Omega = 13\,\mathrm{rad/s}$. The family has been computed by the path-following described in Section 5, starting from the solution with zero amplitude of $\tilde{\theta}$. The periodic functions $\tilde{\theta}_1$ and $\tilde{y}_1$ are discretized by six (complex) Fourier modes. Panel (c) shows the maximum of the periodic orbit depending on the parameter a in a one-parameter bifurcation diagram. The family emerges 'backwards' from the period doubling (at 0.013 m), which shows that the period doubling is subcritical. The family is unstable initially until it folds back at a saddle-node bifurcation (at 0.008 m) where it becomes stable. Path-following is able to find the periodic orbits independently of their dynamical stability in the original emulated system (2)–(3). In fact, the dynamical stability of the orbit is not detected along the curve; it was concluded from the position of the orbit in the bifurcation diagram, relative to the fold point. Fig. 4 (a) and (b)

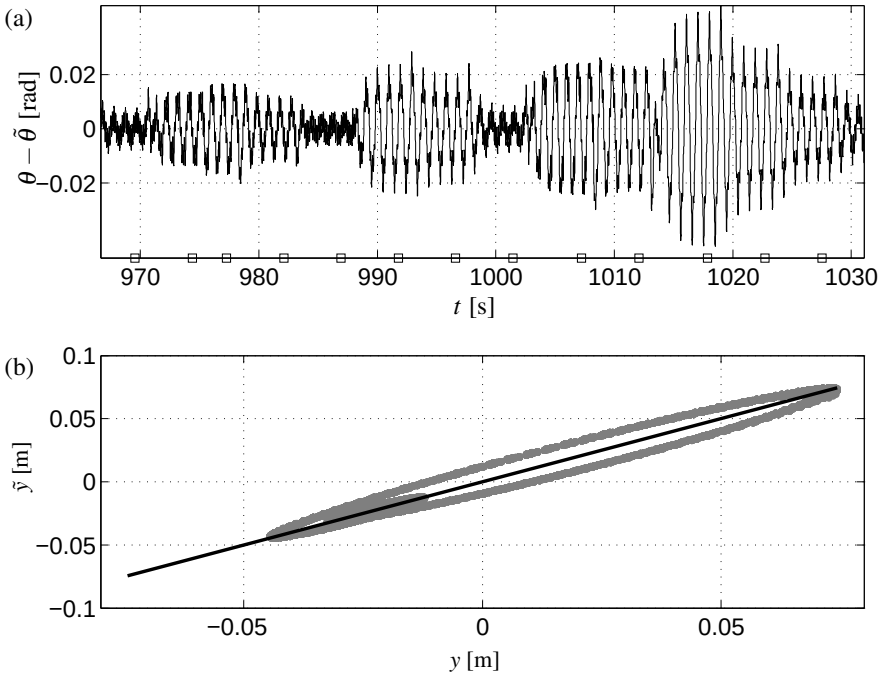

Fig. 5. Illustration of the Quasi-Newton iteration during path-following. Panel (a) shows the time profile of the Quasi-Newton iteration (along the branch shown in Fig. 4(c) for a forcing parameter near 0.02), that is, successively changing inputs until the control input $\theta - \tilde{\theta}$ becomes small. The small squares at the bottom of panel (a) indicate when the outputs θ, y and y_a have settled to a periodic motion. Panel (b) shows the mismatch between actuator input $\tilde{y}$ and output y_a.

show the time profiles of $\tilde{\theta}$ and $\tilde{y}$ (on the interval $[0, 4\pi/\Omega]$) in a waterfall plot. The gray profiles correspond to the unstable part of the family, the black profiles lie on the stable part. The profile of the saddle-node orbit is highlighted in boldface; it separates the stable and unstable parts of the branch.

Fig. 5 (a) shows a typical time profile of the feedback control input $\theta - \tilde{\theta}$ during the path-following along the curve in Fig. 4(c). Note that the transients, occurring whenever $\tilde{\theta}$, $\tilde{y}$ and a are changed, are typically small because these inputs are varied only gradually during the continuation. The squares along the time axis indicate when the system is considered to have settled down to a periodic state. At these time points the last period of the outputs θ, y, and y_a is recorded for the evaluation of the right-hand-sides of (25) and (24), and new inputs and parameters are set. Fig. 5 (b) shows the offset between y and $\tilde{y}$ in the $(y, \tilde{y})$-plane. This offset highlights how much $\tilde{y}$ anticipates the output y of the simulation. Importantly, we achieve synchronization without expressly exploiting the knowledge about the actuator model (6).

7 Conclusion and outlook

We demonstrated with the substructured pendulum-MSD system as a proof-of-concept hybrid experiment that control-based bifurcation analysis is feasible even when the substructured system suffers from delay-induced essential instability. The proposed method does not rely on a particular model for the transfer system connecting the computer simulation and the experiment. It is able to deal with arbitrary unknown actuator dynamics, most notably, it compensates the effect of delay in the actuation. This is in contrast to classic delay compensation schemes, which are not able to overcome an essential instability. The incorporation of control-based bifurcation analysis into the hybrid experiment of the pendulum-MSD system itself is currently in preparation.

As is explained in [8] our approach is general: it allows for systematic bifurcation analysis in experiments that have a stabilizing feedback loop. The underlying idea is to relax the coupling between the two components, so that the experimental subsystem is periodically driven and feedback stabilized with a suitable control input. The condition that the control target be equal to the actual output of the experimental subsystem can be solved iteratively by Newton iteration. One function evaluation corresponds in this context to running the experiment until the system has settled down in response to the prescribed input. Non-invasive control and perfect synchronization correspond to the reproduction of the dynamics of the emulated system. The iterative nature of our method removes the real-time constraint for the numerical component of the overall hybrid test. Therefore, control-based bifurcation analysis may be particularly useful in situations when the numerical component is so complex that its evaluation is too time-consuming to satisfy real-time constraints.

Apart from the experimental validation of our proposed methodology, there are a number of other challenges for future research. We mention here the incorporation of other bifurcations, such as the saddle-node bifurcation or torus bifurcation (some bifurcations have been studied in [8]), the detection of bifurcations along families of periodic solutions, and the development of methods for strongly nonlinear phenomena (such as homoclinic orbits).

Acknowledgments

The authors thank Alicia Gonzalez-Buelga, Yuliya Kyrychko, Simon Neild and David Wagg for helpful discussion on hybrid testing and the pendulum-MSD experiment.

References

[1] J. Guckenheimer, P. Holmes, Nonlinear Oscillations, Dynamical Systems, and Bifurcations of Vector Fields, Springer Verlag, 1983.

[2] Y. Kuznetsov, Elements of Applied Bifurcation Theory, Springer Verlag, 2004, third edition.

[3] W. Govaerts, Y. Kuznetsov, Interactive continuation tools, in: B. Krauskopf, H. Osinga, J. Galán-Vioque (Eds.), Numerical Continuation Methods for Dynamical Systems: Path following and boundary value problems, Springer-Verlag, Dordrecht, 2007, pp. 51–75.

[4] A. Blakeborough, M. Williams, A. Darby, D. Williams, The development of real-time substructure testing, Philosophical Transactions of the Royal Society of London A 359 (2001) 1869–1891.

[5] M. Wallace, D. Wagg, S. Neild, An adaptive polynomial based forward prediction algorithm for multi-actuator real-time dynamic substructuring, Proceedings of the Royal Society of London A 461 (2005) 3807–3826.

[6] Y. Kyrychko, K. Blyuss, A. Gonzalez-Buelga, S. Hogan, D. Wagg, Real-time dynamic substructuring in a coupled oscillator-pendulum system, Proc. Roy. Soc. London A 462 (2006) 1271–1294.

[7] A. Gonzalez-Buelga, D. Wagg, S. Neild, Parametric variation of a coupled pendulum-oscillator system using real-time dynamic substructuring, Structural Control and Health Monitoring (in press), published online at `http://dx.doi.org/10.1002/stc.189`.

[8] J. Sieber, B. Krauskopf, Control based bifurcation analysis for experiments, Nonlinear Dynamics (in press), online first at `http://dx.doi.org/10.1007/s11071-007-9217-2`.

[9] J. Sieber, B. Krauskopf, Control-based continuation of periodic orbits with a time-delayed difference scheme, Int. J. of Bifurcation and Chaos (in press), (`http://hdl.handle.net/1983/399`).

[10] M. Nakashima, Development, potential and limitations of real-time online (pseudo dynamic) testing, Phil. Trans. Roy. Soc. A 359 (2001) 1851–1867.

[11] E. J. Doedel, A. R. Champneys, T. F. Fairgrieve, Y. A. Kuznetsov, B. Sandstede, X. Wang, AUTO97, Continuation and bifurcation software for ordinary differential equations, Concordia University (1998).

[12] E. Doedel, Lecture notes on numerical analysis of nonlinear equations, in: B. Krauskopf, H. Osinga, J. Galán-Vioque (Eds.), Numerical Continuation Methods for Dynamical Systems: Path following and boundary value problems, Springer-Verlag, Dordrecht, 2007, pp. 51–75.

[13] M. Wallace, J. Sieber, S. Neild, D. Wagg, B. Krauskopf, Stability analysis of real-time dynamic substructuring using delay differential equation models, Int. J. of Earthquake Engineering and Structural Dynamics 34 (15) (2005) 1817–1832.

[14] T. Horiuchi, T. Konno, A new method for compensating actuator delay in real-time hybrid experiments, Philosophical Transactions of the Royal Society A 359 (2001) 1893–1909.

[15] A. Darby, A. Blakeborough, M. Williams, Improved control algorithm for real-time substructure testing, Int. J. of Earthquake Engineering and Structural Dynamics 30 (2001) 431–448.

[16] A. Darby, M. Williams, A. Blakeborough, Stability and delay compensation for real-time substructure testing, J. of Engrg. Mech. 128 (2002) 1276–1284.

[17] J. Hale, S. Verduyn Lunel, Introduction to Functional Differential Equations, Springer-Verlag, 1993.

[18] O. Diekmann, S. van Gils, S. V. Lunel, H.-O. Walther, Delay Equations, Springer-Verlag, 1995.

[19] A. Pazy, Semigroups of Linear Operators and Applications to Partial Differential Equations, Springer Verlag, 1983.

[20] Q. Wang, T. Lee, K. Tan, Finite spectrum assignment for time-delay systems, Springer Verlag, 1999.

[21] T. Insperger, Act-and-wait concept for continuous-time control systems with feedback delay, IEEE Transactions on Control Systems Technology 14 (5) (2006) 974–977.

[22] J. Sieber, Dynamics of delayed relay systems, Nonlinearity 19 (11) (2006) 2489–2527.

[23] V. Eyert, A comparative study on methods for convergence acceleration of iterative vector sequences, Journal of Computational Physics 124 (0059) (1996) 271–285.